Beyond the Third Dimension: How Multidimensional Projections and Machine Learning Can Help Each Other

Alexandru Telea[a]
Department of Information and Computing Science, Utrecht University, Netherlands

Keywords: Multidimensional Projections, Visual Quality Metrics, Explainable AI.

Abstract: Dimensionality reduction (DR) methods, also called projections, are one of the techniques of choice for visually exploring large high-dimensional datasets. In parallel, machine learning (ML) and in particular deep learning applications are one of the most prominent generators of large, high-dimensional, and complex datasets which need visual exploration. As such, it is not surprising that DR methods have been often used to open the black box of ML methods. In this paper, we explore the synergy between developing better DR methods and using them to understand and engineer better ML models. Specific topics covered address selecting suitable DR methods from the wide arena of such available techniques; using ML to create better, faster, and simpler to use direct and inverse projections; extending the projection metaphor to create dense representations of classifiers; and using projections not only to explain, but also to improve, ML models. We end by proposing several high-impact directions for future work that exploit the outlined ML-DR synergy.

1 INTRODUCTION

Machine learning (ML) techniques support tasks such as classification and regression and have become fundamental instruments in daily practice in a myriad of fields. Developments in the past decade have made such techniques increasingly accurate, computationally scalable, but most importantly, able to address efficiently and effectively an increasing range of problems such as image analysis (*e.g.*, classification, segmentation, and restoration), sentiment identification, natural language processing, to mention just a few. The advent of deep learning (DL) techniques coupled with recent advances in GPU and parallel computing has massively simplified the ease of creating trained ML models to solve these problems at industrial scale.

Dimensionality reduction (DR), also called projection, is a popular technique for visualizing high-dimensional datasets by low-dimensional scatterplots. Globally put, a good projection scatterplot captures well the so-called *data structure* present in the original high-dimensional data in terms of point clusters, outliers, and correlations (Nonato and Aupetit, 2018; Espadoto et al., 2019a; Lespinats and Aupetit, 2011). As such, high-quality projections allow users to reason about the data structure by exploring the visual structure of the low-dimensional scatterplots they produce. Tens of different DR techniques (Espadoto et al., 2019a) have been designed to address the several requirements one has for this class of methods, such as computational scalability, ease of use, stability *vs* noise or small data changes, projecting additional points along those existing in an original dataset (out-of-sample ability), and visual quality that preserves the high-dimensional data structure.

ML and DR techniques, while having emerged from different fields, share a key similarity: They both deal with *high-dimensional data* – a challenging endeavor. In ML, such data are the so-called features used during training and inference by models. In DR, such data represent the samples, or observations, whose data structure we aim to understand by means of low-dimensional scatterplots. The two fields also share other important commonalities: ML strongly needs methods to open up the 'black box' formed by architecting, training, and using the models it creates, and many such models are visual, like the DR scatterplots. Conversely, the task of creating high-quality projections from high-dimensional data, with guaranteed stability, out-of-sample ability, generalizability, and computational scalability shares all typical requirements met by ML engineering.

In this paper (and related talk), we aim to provide an overview of the research at the crossroads of ML and DR with a particular emphasis on highlighting commonalities between the two fields and recent ways in which they can benefit from each oth-

[a] https://orcid.org/0000-0003-0750-0502

Telea, A.
Beyond the Third Dimension: How Multidimensional Projections and Machine Learning Can Help Each Other.
DOI: 10.5220/0011926400003417
In *Proceedings of the 18th International Joint Conference on Computer Vision, Imaging and Computer Graphics Theory and Applications (VISIGRAPP 2023) - Volume 5: VISAPP*, pages 5-16
ISBN: 978-989-758-634-7; ISSN: 2184-4321

ers' advances. We start by a short overview of ML and DR that outlines common aspects of these two fields (Sec. 2). We next outline how DR methods are used to assist ML engineering tasks (Sec. 3). Next, we discuss how the converse fertilization occurs, namely ML methods being used to create better DR techniques (Sec. 4). Section 5 merges the insights of the previous two sections and outlines high-potential future research directions in which the DR and ML fields can benefit from each other. Finally, Section 6 concludes the paper.

2 BACKGROUND

Providing a full introduction of both ML and DR is out of scope of thos paper. This section aims to provide a brief outline of the key concepts in the two fields which are needed to follow the further discussion and, importantly, highlight commonalities of ML with DR that next lead to cross-fertilization.

2.1 Machine Learning

We start by listing some notations. Let $D = \{\mathbf{x}_i\}$ be a dataset of N-dimensional samples or points $\mathbf{x}_i$, $1 \leq i \leq N$. A point $\mathbf{x}_i = (x_i^1, \ldots, x_i^n)$ consist of n components x_i^j, also called feature or attribute values. Without generality loss, we assume next for simplicity that each of these is a real-value, *i.e.*, $\mathbf{x}_i \in \mathbb{R}^n$. The sets $X^j = (x_1^j, \ldots, x_N^j)$, $1 \leq i \leq N$ are called the features, or dimensions, of the entire dataset D. Simply put, D can be seen as a table having N rows (one per sample) and n columns (one per dimension). An *annotated* dataset D_a associates an additional value $y_i \in A$ to each sample $\mathbf{x}_i$ of a given dataset D.

Machine learning aims to create so-called *models* $f : \mathbb{R}^n \rightarrow A$ which, when applied to a so-called test set $D_T \subset D_a$, deliver the expected annotations, *i.e.*, $d(f(\mathbf{x}_i), y_i) \simeq 0$, for ideally all $\mathbf{x}_i \in D_T$. Here, $d : A \times A \rightarrow \mathbb{R}^+$ is a distance function used to compare the so-called ground-truth annotations y_i with the model's predictions $f(\mathbf{x}_i)$, *e.g.*, an L_p norm. Models f are built by using a so-called training set $D_t \subset D_a$, $D_t \cap D_T = \varnothing$, to adjust f's parameters so as to achieve the above-mentioned goal. Two main types of models exist in ML. *Classifiers* use an annotation set having categorical values (also called labels), in which case one strives for $d = 0$. *Regressors* use an annotation set having real values (in one or more dimensions), in which case one strives for $d \simeq 0$.

Many methods exist to measure the performance of ML models. The most widespread such methods measure several so-called quality metrics on the training set (training performance) and, separately, on the unseen test set (testing performance). Common metrics include accuracy, precision, recall, F-score, and Cohen's kappa score. More advanced methods take into account hyperparameters that allow optimizing between precision and recall, *e.g.* the Receiver Operator Characteristic (ROC) curve and area underneath. Recent surveys of such metrics and related benchmarks are given in (Botchkarev, 2019; Jiang et al., 2020; Thiyagalingam et al., 2022).

2.2 Dimensionality Reduction

Consider a high-dimensional dataset D defined as for the ML context (Sec. 2.1). A dimensionality reduction technique, or projection P, is a function that maps D to $P(D) = \{\mathbf{y}_i\}$, where $\mathbf{y}_i \in \mathbb{R}^q$ is the projection of $\mathbf{x}_i$. Typically $q \ll n$, yielding 2D projections ($q = 2$) and 3D projections ($q = 3$) that are used to visualize D by depicting the respective scatterplots. Projections aim to preserve the so-called *structure* of the dataset D. Intuitively put, this means that patterns in D such as clusters of densely packed points, outliers, and gaps between such point formations, should be visible in $P(D)$.

How well a projection preserves data structure is measured by several quality metrics. A quality metric is a function $M(D, P(D)) \rightarrow \mathbb{R}^+$ that tells how well the scatterplot $P(D)$ captures aspects of the dataset D. Such metrics can be roughly divided into those that measure *distance* preservation between $\mathbb{R}^n$ and $\mathbb{R}^2$, such as normalized stress and the Shepard diagram correlation; and metrics that look at how well (small) neighborhoods of points are preserved between D and $P(D)$, such as trustworthiness, continuity, or, more specific ones, *e.g.* Kullback-Leibler divergence. Extensive surveys of projection quality metrics are given in (Nonato and Aupetit, 2018; Espadoto et al., 2019a).

2.3 Common Sspects of ML and DR

Tens, if not hundreds, of algorithms and techniques have been proposed for both ML and DR. As our goal is to highlight ways in which ML can help DR (and conversely), we next do not discuss such specific algorithms in detail. Rather, we focus our analysis on *common* aspects of the two fields. To this end, it is already important to note that both ML models f and DR projection methods P can be seen as specialized cases of *inference*. More specifically, P can be seen as a particular type of regressor from $\mathbb{R}^n$ to $\mathbb{R}^2$. Given this, we next use the notation X to jointly denote an ML model or DR algorithm, when distinguishing be-

tween the two is not important.

Without claiming full coverage, we identify the following key aspects that both ML and DR techniques X strive to achieve:

Genericity. X should be readily applicable to any dataset D – that is, of any dimensionality, attribute types, and provenance application domain.

Accuracy. X should deliver highly accurate results (inferences for ML; projection scatterplots for DR) as gauged by specific quality metrics in the two fields.

Scalability. X should scale well computationally with the number of samples N and dimensions n – ideally, X should be linear in both N and n. In practice, X should be readily able to handle datasets with millions of samples and hundreds of dimensions on commodity hardware at interactive rates. This further on enables the use of X in *visual analytics* scenarios where the iterative and interactive exploration of complex hypotheses via data visualization is essential.

Out of Sample (OOS). An operator X is said to be OOS if it can extrapolate its behavior beyond the data from which it was constructed. In ML, this usually means that the model f extrapolates from a training set D_t to an unseen test set D_T and beyond. By analogy, a projection P is OOS if, when extending some dataset D with additional samples D', the projection $P(D \cup D')$ ideally keeps the points originally in D at the locations they had in $P(D)$, *i.e.*, $P(D \cup D') = P(D) \cup P(D')$. This is essential in scenarios where one has a growing dataset to be projected. *Existing* points should not change their *existing* projection locations if we want to help users maintain their mental map when interpreting the projection. As most ML methods are OOS by design, they can be potentially used to design OOS projections (Sec. 4).

Stability. Small changes in the input dataset D should only lead to small changes in the output dataset $X(D)$. If not, then noise-level perturbations in D will massively affect the resulting inference $X(D)$ thereby rendering such results potentially unusable and/or misleading. Note that stability is related but not the same as OOS: An OOS algorithm needs to be stable by definition but not all stable algorithms have OOS ability (Vernier et al., 2021; Espadoto et al., 2019a). Similarly, large-scale changes in D should arguably lead to correspondingly large changes in $X(D)$. We discuss this aspect in more detail when outlining the challenges of dynamic projections (Sec. 5.2).

Availability. X should be readily available to practitioners in terms of documented open-source code. While sometimes neglected, this is a key requirement for ML and DR algorithms to become impactful in practice.

Most ML techniques in existence comply by design with the above properties. However, not all DR techniques do the same. As we shall see in Sec. 4, ML can be used to construct DR techniques, thereby making the latter techniques inherit all the desirable properties of the former.

3 DR FOR ASSISTING ML

Given the close relation between DR and ML outlined above, it is not surprising that DR has been used as a visual analysis tool to assist model engineering. We next discuss several prominent cases of such usage of DR.

3.1 Assessing and Improving Classifiers

Arguably the most frequent use of DR for ML engineering is to create a projection of a training or test set, with points colored by class and/or correct-*vs*-wrong classification, and use it to assess the model's working. Indeed, since (a) a projection places similar samples close to each other and (b) a classifier labels similar samples similarly, then the visual structure of the projection should convey insights on how *easily separable* are samples of different classes. While this intuition has been long used, it is only recently that a formal study of this correlation was presented (Rauber et al., 2017b). In the respective work, the authors show that a dataset D which creates a projection $P(D)$ in which classes are well separated (as measured *e.g.* by the neighborhood hit metric) will be far easier classifiable than a dataset whose projection shows intermixed points of different labels. The projection $P(D)$ thus becomes a 'proxy' for the ease of classifying D *regardless* of the type of classifier being used. This helps one in assessing classification difficulty *before* actually embarking in the expensive cycle of classifier design-train-test.

Figure 1 illustrates the above. Images (a) and (b) show the two-class Madelon dataset (Guyon et al., 2004) ($n = 500$ features) classifier by KNN and Random Forests (RFC) respectively, with samples projected by t-SNE (van der Maaten and Hinton, 2008) and colored by class. The two projections show a very poor separation of the two classes, in line with the obtained accuracies $AC = 54\%$ and $AC = 66\%$. Images (c) and (d) show the same dataset where extremely randomized trees (Geurts et al., 2006) was used to select $n = 20$ features. The projections show a much higher visual separation of the two classes, in line with the obtained accuracies $AC = 88\%$ and $AC = 89\%$. Numerous other examples in (Rauber

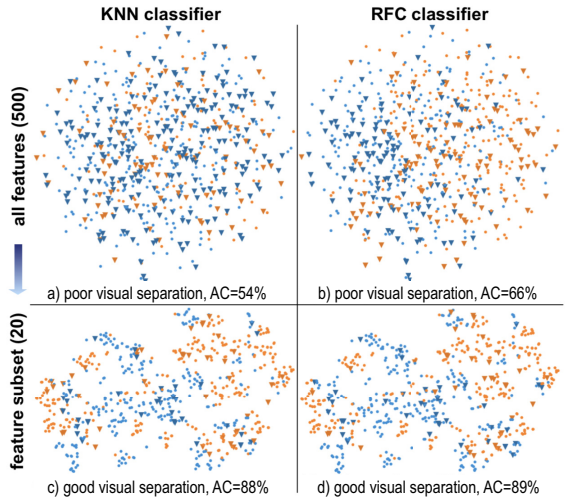

Figure 1: Classification difficulty assessment via projections (Rauber et al., 2017b).

et al., 2017b) show that projections are good predictors of classification difficulty.

3.2 Pseudolabeling for ML Training

If projections are good predictors for classification accuracy, it means that their low-dimensional (2D) space captures well the similarity of the high-dimensional samples. Following this, the next step is to actually *use* projections to engineer classifier models. A first attempt was shown by (Benato et al., 2018) for the task of training a classifier from a training set having only very few labeled points: The entire training set, including unlabeled points, is projected and the user explores the projection to find unlabeled points tightly packed around labeled ones. Following visual confirmation that the packed samples are of the same class as the surrounded label (using a tooltip to look at the image samples), the user selects the former and assigns them the latter's label. The process quickly leads to sufficiently large labeled sets for training the desired model. More interestingly, *automated* label propagation in the embedded space using state-of-the-art methods leads to poorer results than user-driven labeling, which confirms the added value of the human-in-the-loop and thus the projections.

However, the best results are obtained when humans and machine *cooperate* rather than aim to replace each other. (Benato et al., 2020) adapted the above workflow to (a) use an automatic label propagation for the 2D projection points where the propagation confidence is high; and (b) expose the remaining points to manual labeling (see Fig. 2). This way, many 'easy to label' points are handled automatically whereas the user's effort is channeled towards the difficult case. This strategy led to increasing model accuracy and, again, surpassed confidence-based label propagation into the high-dimensional space.

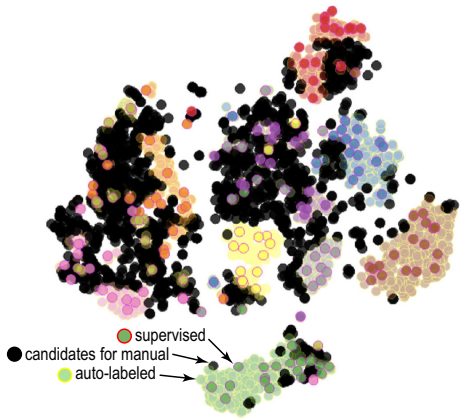

Figure 2: Semi-automatic label propagation for constructing training sets. An algorithm propagates ground-truth labels from a small set of supervised samples towards neighbor samples. When this algorithm is uncertain, samples are left for manual labeling (Benato et al., 2020).

3.3 Understanding DL Models

Projections can be used not only to understand the end-to-end behavior of classifier models but also their *internals*. This become especially useful when we consider deep learned (DL) models which, with their millions of parameters, are among the hardest artifacts in ML to understand. 'Opening the black box' of DL models is one of the most challenging, and also most actual, goals of explainable AI (XAI) (Shwartz-Ziv and Tishby, 2017; Azodi et al., 2020). Visualization has been listed early on as the technique of choice for this endeavor (Tzeng and Ma, 2005). A recent surve (Garcia et al., 2018) outlines a wide spectrum of visual analytics techniques and tools used for DL engineering, classified in terms of supporting the tasks of training analysis (TA), architecture understanding (AU), and feature understanding (FU). Given the diversity of these tasks, the variety of the proposed visual analytocs solutions – *e.g.* matrix plots, icicle plots, parallel coordinate plots, stacked barcharts, annotated networks, activation maps – is not surprising.

Projections occupy a particular role among these visualizations due to their ability to compactly capture high-dimensional data – in the limit, a projection needs a single pixel to represent an n-dimensional point, for any n value. As such, they are very suitable instruments to depict several aspect of a DL model. For example, in Fig. 3a, every point denotes a high-dimensional sample, in this case a digit image from the SVHN dataset (Rauber et al., 2017b). The points,

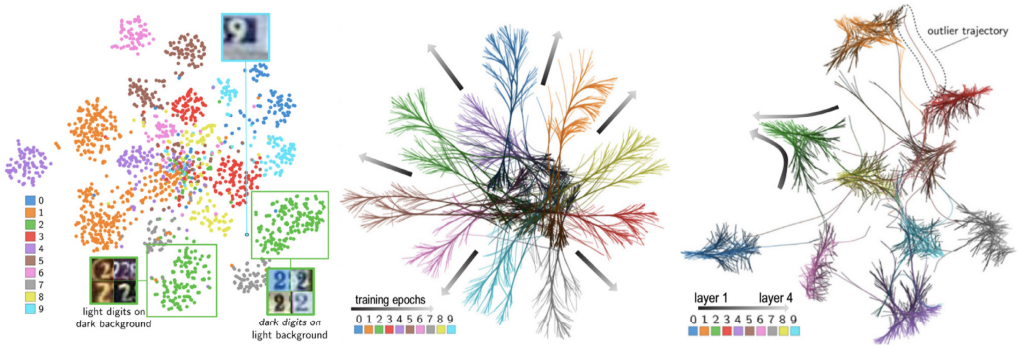

a) explore learned features b) explore training *vs* time c) explore training *vs* layers

Figure 3: Projections for understanding DL models. Exploring (a) activations of similar instances, (b) evolution of activations over training epochs, and (c) evolution of activations over network layers (Rauber et al., 2017a).

colored by their ground-truth class, have as dimensions all activations of the last hidden layer of a DL model created to classify this dataset. We notice a good separation of same-class images, which tells that the model was successfully trained. We also see two clusters of same-class points, which tell that the model has learned to split images of the *same* digit into two subclasses. Upon inspection, we see that the model has learned *by itself* to separate dark-on-bright-background digits from bright-on-dark background ones. Such findings would not be possible without the insights given by visual tools such as projections. Moreover, such findings can help the ML engineers to fine-tune their models to increase performance – in this case, eliminate the 'color contrast learning' which does not help the targeted classification. Figure 3b explores a different DL aspect, namely how the model learns. For every epoch, a projection of all training-set samples is made of the samples' last hidden layer activations, similar to image (a). To maintain temporal coherence, *i.e.*, have similar-value samples project to close locations over the entire set of epochs, a *dynamic* projection algorithm, in this case dt-SNE (Rauber et al., 2016), was used. Next, same-image points from all epochs are connected by a trail. As the last step, trails are bundled in 2D (van der Zwan et al., 2016) to reduce visual clutter. The resulting image shows how the projection literally fans out from a dark clump (in the middle of the image), where last-layer neurons exhibit similar activations for all images, to separated clusters of same-label images. This effectively summarizes the training success – we see, for example, that the purple bundle (digit 4) is less well separated from the others, which indicates some challenges in classifying this digit. Finally, Fig. 3c shows a similarly-constructed visualization but where the trails connect projections of test-set image activations through all network's hidden *layers*. Bundles, initially dark and wide (layer 1), fan in, indicating that the network progressively separates images of different classes as the data flows through its layers – *i.e.*, that the network architecture is indeed good for the classification task at hand.

3.4 Decision Boundary Maps

All projections shown so far visualize a *discrete* set D of samples processed by a ML model f. However, such models are, in general, designed to accept samples from a dense set $Z \subset \mathbb{R}^n$. Classifiers, for instance, partition Z into so-called *decision zones* (dense sets in Z whose points get the same label) separated by *decision boundaries*. Such decision boundaries are in general complex manifolds embedded into $\mathbb{R}^n$ and were, until recently, only depictable for very simple models such as logistic regression. Ideally, the ML engineer would like to see how f behaves on the entire dense space Z and not only on the *sparse* sampling thereof given by training (D_t) or test (D_T) sets.

Since projections perform so well for visually exploring classifiers, it makes sense to consider extending them to depict decision zones and boundaries. Intuitively put, such boundaries would go through the whitespace in a projection to separate the same-color point clusters in *e.g.* Fig. 3a. Seeing decision zones and boundaries and their relations to training and/or test samples would help ML engineers to *e.g.* find where in the input space more training samples are needed to improve a classifier or, conversely, assess in which such areas would samples be misclassified.

Decision boundary maps (DBMs) propose such a visual representation for both decision zones and boundaries for any classifier. Intuitively put, DBMs map the entire space Z (as classified by f) to 2D rather than the discrete sample set D, as follows. Given an image space $I \subset \mathbb{R}^2$, a mapping $P^{-1} : I \rightarrow \mathbb{R}^n$ is constructed to 'backproject' each pixel $\mathbf{y} \in I$ to a high-

dimensional point $\mathbf{x} = P^{-1}(\mathbf{y})$. Next, $\mathbf{y}$ is colored by the label $f(\mathbf{x})$ assigned to it by a trained classifier to be explored. Same-color areas emerging in I indicate f's decision zones; pixels on the frontiers of these areas show f's decision boundaries. The key to DBM construction is creating the mapping P^{-1}. One way to do this, shown in Fig. 4a, is to use distance-based interpolation over the points $P(D)$ of a parametric (that is, OOS) projection of the training and/or test set of f (Schulz et al., 2015; Schulz et al., 2020). Another way, shown in Fig. 4b, is to general purpose so-called *inverse projection* techniques (Rodrigues et al., 2018). Finally, one can construct P^{-1} by using deep learning (Fig. 4c), as discussed further in Sec. 4.2.

DBMs can be further enhanced to encode, via brightness, the classifier's confidence at every 2D pixel (Figs. 4a,c) or actual n-dimensional distance to the closest decision boundary (Fig. 4b). The appearing brightness gradients tell which areas in the projection space are more prone to misclassifications. Importantly, this does not require actual samples to exist in a training or test set in these areas – rather, such samples are synthesized by P^{-1}.

4 ML FOR ASSISTING DR

Section 3 has shown several examples of the added value of projections for ML engineering. However, as noted in Sec. 2.3, not all projection techniques satisfy all desirable requirements needed for them to be readily used in ML visualization (and, actually, in other contexts as well). An important question is thus: Which projection techniques are the best candidates for such use-cases?

A recent survey (Espadoto et al., 2019a) addressed this question at scale for the first time by comparing 44 projection techniques P over 19 datasets D from the perspective of 6 quality metrics M, using grid-search to explore the hyperparameter spaces of the projection techniques. This is to date the only large-scale survey that quantitatively assesses DR methods over many datasets, techniques, quality metrics, and parameter settings. Equally important, all its results – datasets, projection techniques, quality metric implementations, study protocol – are automated and freely available, much like similar endeavors in the ML arena. Following the survey's results, four projection methods consistently scored high on quality for all datasets (UMAP (McInnes et al., 2018), t-SNE (van der Maaten and Hinton, 2008), IDMAP (Minghim et al., 2006), and PBC (Paulovich and Minghim, 2006)), with several others close to them. However, none of the top-ranked surveyed techniques also met the OOS, computational scalability, and stability criteria. As such, we can conclude that better DR techniques are needed.

4.1 Deep Learning Projections

Following the analogy with ML regressors (Sec. 2.3, it becomes interesting to consider ML for building better projection algorithms. Autoencoders (Hinton and Salakhutdinov, 2006) do precisely that and meet all requirements in Sec. 2.3 except quality – the resulting projections have in general poorer trustworthiness and continuity than state-of-the-art methods like UMAP and t-SNE. Figure 5 illustrates this: The well-known MNIST dataset, which is well separable into its 10 classes by many ML techniques, appears, wrongly, poorly separated when projected by autoencoders. Following (Rauber et al., 2017b) (see also Sec. 3.1, we can conclude that autoencoders are a poor solution for DR.

Recently, Espadoto *et al.* (Espadoto et al., 2020) proposed Neural Network Projections (NNP), a supervised approach to learning DR: Given any dataset D and its projection $P(D)$ computed by the user's technique of choice P, a simple three-layer fully-connected network is trained to learn to regress $P(D)$ when given D. Despite its simplicity, NNP can learn to imitate any projection technique P for any dataset D surprisingly well. While NNP's quality is typically slightly lower than state-of-the-art projections like t-SNE and UMAP, it is a *parametric* method, stable as proven by sensitivity analysis studies (Bredius et al., 2022), OOS, linear in the sample count N and dimensionality n (in practice, thousands of times faster than t-SNE), and very simple to implement.

Figure 6 shows an example of the above-mentioned sensitivity analysis. An NNP model is trained to project the MNIST dataset, after which is asked to project MNIST images where an increasingly larger number of dimensions (pixel values) have been cancelled, *i.e.*, set to zero. Surprisingly, NNP can capture the cluster structure of the data (10 classes for the 10 digits) up to 40% cancelled dimensions. The aggregated image shows the 'movement' of the points in the NNP projection as increasingly more dimensions get dropped. Similar insights are obtained for other input-dataset perturbations such as sample jitter, translation, and scaling. At a higher level, we see sensitivity analysis as a very powerful, yet under-explored, technique – well known in the ML repertoire – to assess the quality of DR projections.

Subsequent refinements included k-NNP (Modrakowski et al., 2021) which enhances quality by learning to project sets of neighbor sam-

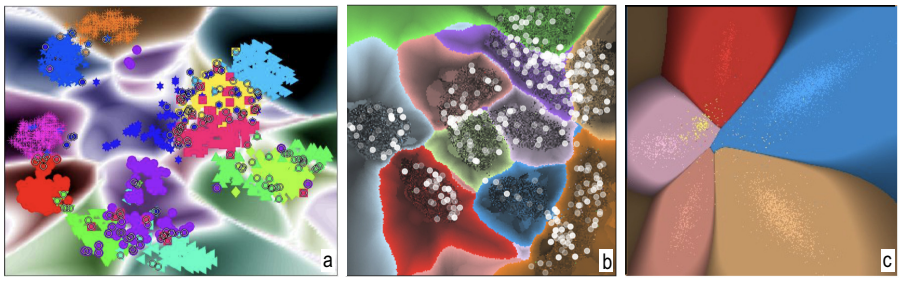

Figure 4: Decision boundary maps for classifier analysis with luminance encoding classifier confidence (a,c) (Schulz et al., 2015; Rodrigues et al., 2019), respectively distance-to-decision-boundary (c) (Oliveira et al., 2022).

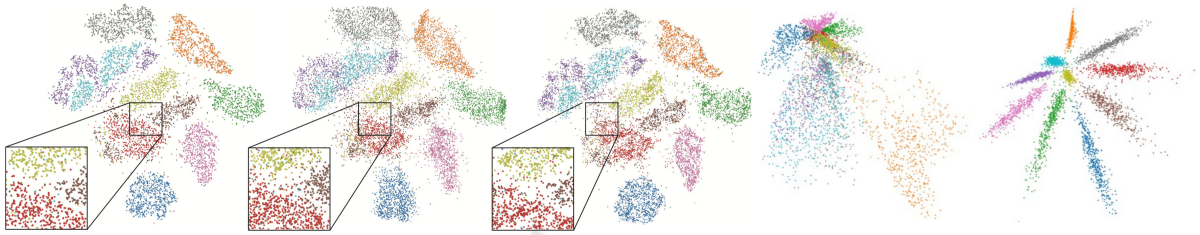

Figure 5: Projection of MNIST dataset with (a) t-SNE (van der Maaten and Hinton, 2008) and with deep learning methods: (b) NNP (Espadoto et al., 2020), (c) kNNP (Modrakowski et al., 2021), (d) autoencoders (Hinton and Salakhutdinov, 2006), (e) SSNP (Espadoto et al., 2021b). For supervised methods, (k)NNP succeeds in well imitating t-SNE. For self-supervised methods, SSNP yields better quality than autoencoders.

ples; SSNP (Espadoto et al., 2021b) which works in a self-supervised way, similar to autoencoders, thus dispensing of the need of a training projection and also being able to create inverse projections (see next Sec. 4.2); SDR-NNP (Kim et al., 2022) which increases NNP's quality by pre-sharpening the input training set D_t via mean shift; and HyperNP (Appleby et al., 2022), which learns the behavior of a projection technique P for all its hyperparameter values. Figure 5 shows several of these techniques applied to the well-known MNIST dataset which illustrates the qualitative comments made above. All in all, the above results prove that DL is a serious contender for generating projections that comply with all requirements set forth by practice.

4.2 Deep Learning Inverse Projections

Following the success of DL for constructing projections P outlined above, it becomes immediately interesting to ask if we cannot do the same to construct *inverse* projections P^{-1}. Introduced in Sec. 3.4 for constructing DBMs, inverse projections have additional uses, *e.g.*, generating synthetic samples for data augmentation scenarios.

Espadoto *et al.* (Espadoto et al., 2019b) answered the above question positively by simply 'switching' the input and output of NNP, *i.e.*, given a dataset D that projects to a 2D scatterplot by some technique P, train a regressor to output D when given $P(D)$. This technique, called NNInv, inherits all the desirable properties of NNP (see Sec. 2.3) and also produces higher-quality DBMs than earlier models for P^{-1}. In particular, NNInv – and also SSNP, the other deep-learning technique able to create inverse projections introduced in Sec. 4.1 – are about two orders of magnitude faster than other existing inverse projection techniques such as iLAMP (Amorim et al., 2012) and RBF (Amorim et al., 2015). NNInv was further explored in detail for visual analytics scenarios involving dynamic imputation and exploring ensemble classifiers (Espadoto et al., 2021a). Figure 7 shows the latter use-case: In the image, each pixel is back-projected and ran through a set of nine classifiers, trained to separate classes 1 and 7 from the MNIST dataset. The pixel is then colored to indicate the classifiers' agreement. Deep blue, respectively red, zones show areas where all classifiers agree with class 1, respectively 7. Brighter areas indicate regions of high classifier disagreement – which are thus highly difficult to decide upon and are prime candidates for ML engineering, regardless of the used classifier.

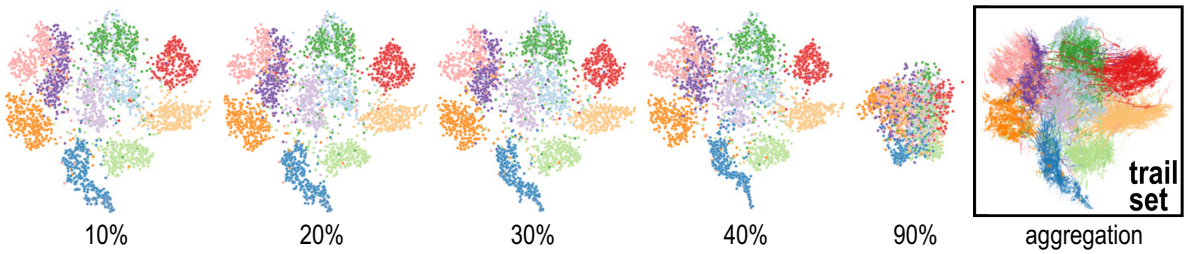

Figure 6: NNP sensitivity analysis when removing between 10% and 90% of the MNIST dimensions. Surprisingly, NNP can robustly depict the data structure even when a large part of the input information is missing (Bredius et al., 2022).

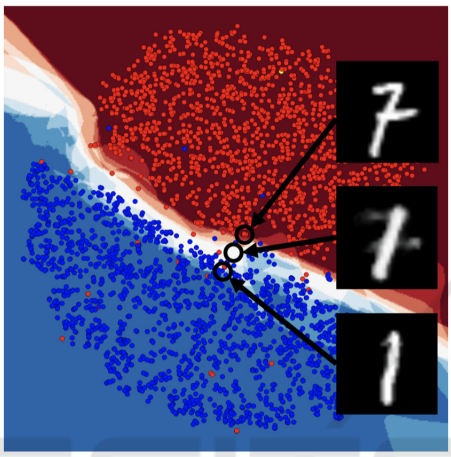

Figure 7: Classifier agreement map for 9 classifiers, MNIST datasets digits 1 and 7. Dark colors indicate more of the 9 classifiers agreeing, at a pixel in the map, with the decision (red=1, blue=7). Brighter, desaturated, colors indicate fewer classifiers in agreement (white=4 classifiers say 1, the other 5 say 7, or conversely) (Espadoto et al., 2021a).

5 THE WAY FORWARD

Figure 8 summarizes the tight interaction between ML and DR described above. The central box (blue) depicts the typical ML pipeline which maps some input real-valued dataset D into class labels or another real-valued signal by means of a classifier, respectively regressor. The box atop this pipeline (green) shows various visualizations that cane used to assist ML engineering, such as semi-automatic labeling (Sec. 3.2), assessing classification difficulty (Sec. 3.1), and assessing training and deep models (Sec. 3.3). The bottom box (yellow) uses ML regressors to build several DR techniques such as (self-)supervised projections (Sec. 4.1) and inverse projections (Sec. 4.2). In turn, these lead to refined visualization methods – sensitivity analysis to assess learned projections (Sec. 4.1) and quality analysis for inverse projections (see Sec. 5.2 further). Finally, all these DR methods can be used to construct the earlier-described visualizations that assist ML engineering (red arrow in Fig. 8).

Reflecting upon the current achievements of using ML for DR and conversely, we see a bright future ahead for research where the two directions strengthen each other. A few selected, non-exhaustive, examples of such potential ML-DR synergies are outlined next.

5.1 Prospects of DR Helping ML

Better DBMs. While current techniques allow the fast creation of accurate DBMs (Sec. 3.4), some fundamental trade-offs still exist. Very accurate techniques exist which solve the inherent ill-posedness of inverting a projection function P which can map different high-dimensional points to the same low-dimensional location (Schulz et al., 2015; Schulz et al., 2020). However, such techniques make various assumptions on the underlying projections, are quite complex to implement, and also computationally expensive – they are far from real-time adaptation of the DBM upon re-training a classifier, which would be ideal for ML engineering (see below). Conversely, DL-based techniques like NNInv and SSNP are near-real-time and simple to implement but may create errors that ultimately mislead their users. We foresee possibilities of using ML, and in particular DL, to improve the latter to match the quality of the former.

DBMs in Use. DBMs are not a goal in themselves, but a tool serving a goal. Apart from the scenarios depicted in (Espadoto et al., 2021a), DBMs could be readily used in a visual analytics explorative scenario to drive a classifier's training. If computable in real-time, users could visualize the DBMs, find problematic areas with respect to how the decision boundaries wrap around samples, and next modify the training set by *e.g.* adding or deleting labels, adding new augmented samples, or even moving samples. We envisage a tool in which users could effectively 'sculpt' the shape of decision boundaries by sample manipulation much as one edits 2D shapes by manipulating spline control points. This would offer unprecedented free-

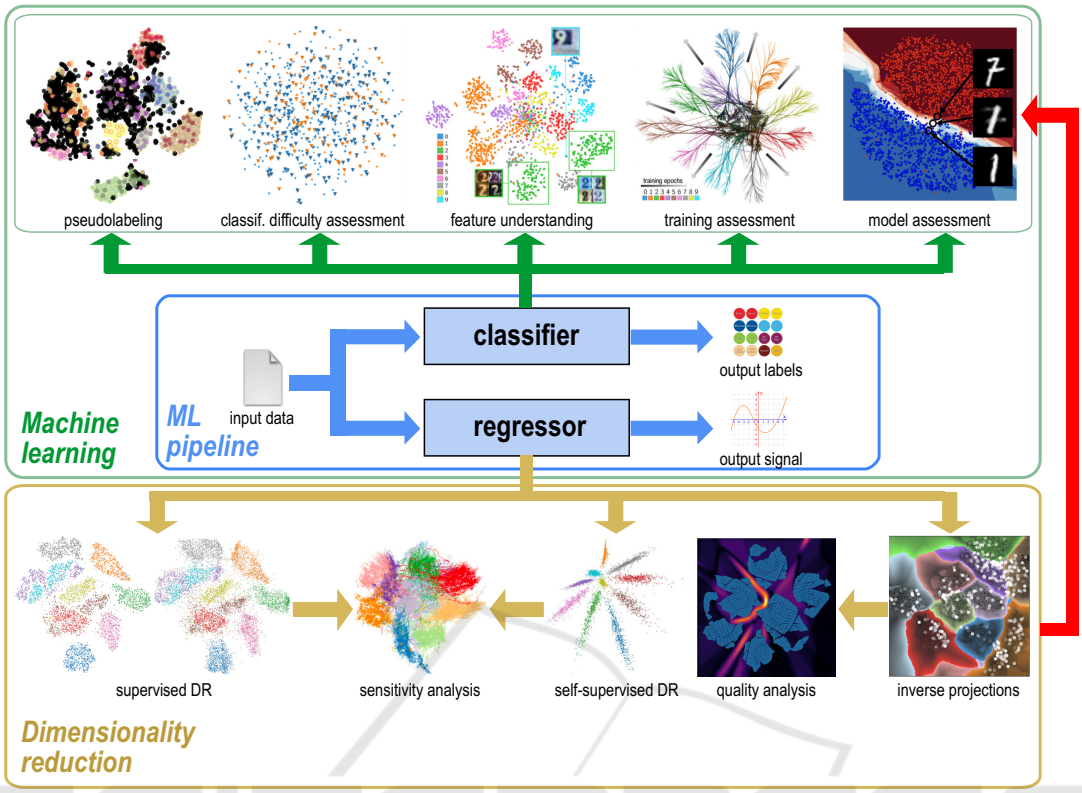

Figure 8: Interactions between machine learning (ML) and dimensionality reduction (DR). See Sec. 5.

dom and a wholly new way of fine-tuning classifiers to extend the approaches pioneered in (Benato et al., 2018; Benato et al., 2020).

Visualizing Regressors. The examples shown in this paper have arguably convinced the reader that projections are efficient and effective in visualizing both high-dimensional data and classifier models working on such data. However, as Sec. 2 mentions, ML is also about a second type of technique, namely *regressors*. A very complex, but high-potential, challenge is to adapt and extend DR methods to visualize regressors (first of the single-variate type, then the multivariate one). This is fundamentally hard as the 2D visual space does not readily offer the possibility of displaying *many* values at a single point. In some sense, it seems that a second DR pass would be needed to reduce the regressor's output dimension to what could be displayed in 2D. Generalizing DBMs from classifiers to 'regressor maps' would open a wide spectrum of possibilities going beyond ML, *e.g.*, in operations research and optimization applications. A recent attempt in this direction was shown in (Espadoto et al., 2021c). However, this approach only treated single-variate regressors $f : \mathbb{R}^n \rightarrow \mathbb{R}$ and used a relatively low-quality projection (PCA).

5.2 Prospects of ML Helping DR

Learning Styles. All current DL-based projection methods use relatively simple cost functions – either aiming to globally mimic a training projection (NNP-class methods) or aiming to globally minimize some reconstruction loss (autoencoder-class methods). A first extension direction would be to refine this loss to *e.g.* create projections where the sizes and/or shapes of clusters can be controlled by data attributes. One high-potential direction would be to create a hierarchy-aware projection algorithm that would combine the advantages of treemaps and classical projections, in the wake of earlier ideas in this class (Duarte et al., 2014). A second extension would be to design *local* cost functions that attempt to construct the projection by combining different criteria for different subsets of the input data – for example, to achieve a globally-better projection that locally behaves like t-SNE in some areas and like UMAP in others. ML techniques can help here by *e.g.* extending the HyperNP idea (Appleby et al., 2022) to train from a set of projection techniques run on the same input dataset. Further inspiration can be gotten from recent ways in which DL is used for image synthesis and style transfer, *e.g.*, (Luan et al., 2017).

Inverse Projection Quality. Only a handful of quality metrics exist to gauge how good inverse projection techniques are (Sec. 4.2). This is not surprising since the main use-case of such tools is to create new data points for locations in the 2D image where no existing data point projects. As such, defining what a good inverse projection should return in such areas is conceptually hard. Yet, possibilities exist. One can *e.g.* use a ML approach where an unseen test set is kept apart from the construction of the inverse projection and is used to assess the quality of such a trained model. For this, suitable distance approximations need to be designed, which can borrow from existing ML approaches to assess regressors. An equally interesting question is how to design a scale, or hierarchy, of errors. It is likely that differently inversely-projected points $\mathbf{x}' = P^{-1}(P(\mathbf{x}))$ that deviate from its ground-truth location $\mathbf{x}$ by the same distance $\|\mathbf{x}' - \mathbf{x}\|$ are not equally good, or equally bad, depending on the application perspective. As such, inverse projection quality metrics may need to be designed in an application-specific way.

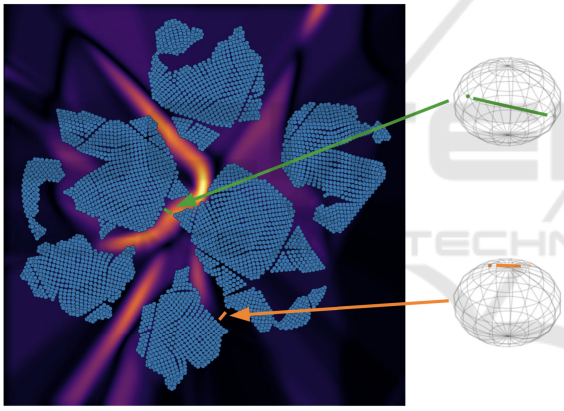

Figure 9: Gradient map of NNInv inverse projection constructing from a t-SNE projection of an uniformly sampled sphere. Hot map regions indicate nearby 2D points that inversely project to far-apart nD points (green line, top sphere). Dark map regions indicate nearby 2D points that inversely project to close nD points (orange line, bottom sphere). The map captures thus the joint projection-inverse projection errors (Espadoto et al., 2021a).

Figure 9 shows another challenge of measuring inverse projection quality. The image shows a so-called gradient map which encodes the gradient magnitude of the P^{-1} function (in this case constructed with NNInv). Hot regions on this map indicate nearby 2D points which backproject far away from each other. However, we cannot directly say that this is an error of the inverse projection P^{-1} – these regions may well correspond to areas where the direct projection P, in this case t-SNE, squeezed faraway data points to fit them in the 2D space – thus areas of low continuity (Venna and Kaski, 2006). It is thus essential, when designing inverse projection errors, to be able to factor out errors induced by the direct projection.

Dynamic Projections. Section 3.3 has briefly introduced dynamic projections. These are extensions of the standard, static, projection techniques which aim to handle a dataset consisting of high-dimensional points which maintain their identity while changing their attribute values through time. Dynamic projections have a wealth of applications – simply put, anywhere one wants to study high-dimensional data which changes over time. However, only a handful of dynamic projection techniques exist (Vernier et al., 2021; Vernier et al., 2020), and their quality – as gauged by established quality metrics – is good in data structure preservation *or* data dynamics preservation but not both aspects. Designing a dynamic projection technique that accurately maps both data structure and dynamics is a grand challenge for the infovis community. Following good recent results in using ML for DR, it looks highly interesting to explore ML (and in particular DL) for creating dynamic projections. A sub-challenge here is that, since good ground-truth dynamic projections are hard to construct, the supervised way (NNP-class methods) may be hard to follow, so the self-supervised direction seems more promising.

6 CONCLUSIONS

For a long time, the research topics of dimensionality reduction (DR) and machine learning (ML) have evolved in parallel and with only tangential encounters. In recent years, however, the two domains have grown increasingly close, spurred by two developments. On the ML side, and largely due to the XAI movement aiming at opening the 'black box' of ML (and in particular deep learning) models, there is increasing awareness and usage of information visualization techniques to explore ML artifacts. On the DR side, increasingly better projection methods in terms of a wide range of quality aspects (*e.g.*, accuracy, speed, stability, to mention just a few) have appeared, which are readily adopted to create new visual tools for ML exploration. More recently, the DR community has also started to adopt ML techniques to create better projection algorithms. Operational difficulties such as poorly scalable and/or hard-to-replicate algorithms are disappearing. As such, all is there for cross-fertilization between ML and DR.

We see this convergence trend which unites research and researchers in DR and ML growing in the

near future, with both areas positively feeding each other in terms of research questions and tasks, and also solutions. A strong common mathematical background also unites researchers in the two fields, making it easy to exchange research questions, ideas, and results. We also see several high-potential research directions at the crossroads of ML and DR: using dense maps to explore and improve classifiers and regressors, effectively mapping the whole high-dimensional space to an image; using ML to create highly customized, high-quality projections for both static and dynamic data; and developing inverse projections to meet all the standards that current direct projection techniques have. Such developments, jointly enabled by DR and ML researchers, will have impact far beyond these two fields.

REFERENCES

Amorim, E., Brazil, E., Daniels, J., Joia, P., Nonato, L., and Sousa, M. (2012). iLAMP: Exploring high-dimensional spacing through backward multidimensional projection. In *Proc. IEEE VAST*.

Amorim, E., Brazil, E., Mena-Chalco, J., Velho, L., Nonato, L. G., Samavati, F., and Sousa, M. (2015). Facing the high-dimensions: Inverse projection with radial basis functions. *Computers & Graphics*, 48:35–47.

Appleby, G., Espadoto, M., Chen, R., Goree, S., Telea, A., Anderson, E., and Chang, R. (2022). HyperNP: Interactive visual exploration of multidimensional projection hyperparameters. *CGF*, 41(3):169–181.

Azodi, C., Tang, J., and Shiu, S. (2020). Opening the black box: Interpretable machine learning for geneticists. *Trends Genet*, 36(6):442–455.

Benato, B., Gomes, J., Telea, A., and Falcão, A. (2020). Semi-automatic data annotation guided by feature space projection. *Pattern Recognition*, 109:107612.

Benato, B., Telea, A., and Falcão, A. (2018). Semi-supervised learning with interactive label propagation guided by feature space projections. In *Proc. SIBGRAPI*, pages 392–399.

Botchkarev, A. (2019). Performance metrics (error measures) in machine learning regression, forecasting and prognostics: Properties and typology. *Interdisciplinary J. of Information, Knowledge, and Management*, 14:45–79.

Bredius, C., Tian, Z., and Telea, A. (2022). Visual exploration of neural network projection stability. In *Proc. MLVis*.

Duarte, F., Sikanski, F., Fatore, F., Fadel, S., and Paulovich, F. V. (2014). Nmap: A novel neighborhood preservation space-filling algorithm. *IEEE TVCG*, 20(12):2063–2071.

Espadoto, M., Appleby, G., A. Suh, D. C., Li, M., Scheidegger, C., Anderson, E., Chang, R., and Telea, A. (2021a). UnProjection: Leveraging inverse-projections for visual analytics of high-dimensional data. *IEEE TVCG*. DOI:10.1109/TVCG.2021.3125576.

Espadoto, M., Hirata, N., and Telea, A. (2020). Deep learning multidimensional projections. *Information Visualization*, 9(3):247–269.

Espadoto, M., Hirata, N., and Telea, A. (2021b). Self-supervised dimensionality reduction with neural networks and pseudo-labeling. In *Proc. IVAPP*.

Espadoto, M., Martins, R., Kerren, A., Hirata, N., and Telea, A. (2019a). Toward a quantitative survey of dimension reduction techniques. *IEEE TVCG*, 27(3):2153–2173.

Espadoto, M., Rodrigues, F. C. M., Hirata, N., and Telea, A. (2021c). OptMap: Using dense maps for visualizing multidimensional optimization problems. In *Proc. IVAPP*.

Espadoto, M., Rodrigues, F. C. M., Hirata, N. S. T., Jr, R. H., and Telea, A. (2019b). Deep learning inverse multidimensional projections. In *Proc. EuroVA*.

Garcia, R., Telea, A., da Silva, B., Torresen, J., and Comba, J. (2018). A task-and-technique centered survey on visual analytics for deep learning model engineering. *Computers and Graphics*, 77:30–49.

Geurts, P., Ernst, D., and Wehenkel, L. (2006). Extremely randomized trees. *Machine learning*, 63(1):3–42.

Guyon, I., S, S. G., and Ben-Hur, A. (2004). Result analysis of the NIPS 2003 feature selection challenge. In *Advances in Neural Information Processing Systems*, page 545?552.

Hinton, G. E. and Salakhutdinov, R. R. (2006). Reducing the dimensionality of data with neural networks. *Science*, 313(5786):504–507.

Jiang, T., Gradus, J., and Rosellini, A. (2020). Supervised machine learning: A brief primer. *Behavior Therapy*, 51(5):675–687.

Kim, Y., Espadoto, M., Trager, S., Roerdink, J., and Telea, A. (2022). SDR-NNP: Sharpened dimensionality reduction with neural networks. In *Proc. IVAPP*.

Lespinats, S. and Aupetit, M. (2011). CheckViz: Sanity check and topological clues for linear and nonlinear mappings. *CGF*, 30(1):113–125.

Luan, F., Paris, S., Shechtman, E., and Bala, K. (2017). Deep photo style transfer. In *Proc. IEEE CVPR*.

McInnes, L., Healy, J., and Melville, J. (2018). UMAP: Uniform manifold approximation and projection for dimension reduction. arXiv:1802.03426v2 [stat.ML].

Minghim, R., Paulovich, F. V., and Lopes, A. A. (2006). Content-based text mapping using multi-dimensional projections for exploration of document collections. In *Proc. SPIE*. Intl. Society for Optics and Photonics.

Modrakowski, T., Espadoto, M., Falcao, A., Hirata, N., and Telea, A. (2021). Improving deep learning projections by neighborhood analysis. In *Communication in Computer and Information*. Springer.

Nonato, L. and Aupetit, M. (2018). Multidimensional projection for visual analytics: Linking techniques with distortions, tasks, and layout enrichment. *IEEE TVCG*.

Oliveira, A. A. M., Espadoto, M., Hirata, R., and Telea, A. (2022). SDBM: Supervised decision boundary maps for machine learning classifiers. In *Proc. IVAPP*.

Paulovich, F. V. and Minghim, R. (2006). Text map explorer: a tool to create and explore document maps. In *Proc. IEEE IV*, pages 245–251.

Rauber, P., Fadel, S. G., Falcão, A., and Telea, A. (2017a). Visualizing the hidden activity of artificial neural networks. *IEEE TVCG*, 23(1):101–110.

Rauber, P., Falcao, A., and Telea, A. (2016). Visualizing time-dependent data using dynamic t-SNE. In *Proc. EuroVis – short papers*, pages 43–49.

Rauber, P. E., Falcão, A. X., and Telea, A. C. (2017b). Projections as visual aids for classification system design. *Inf Vis*, 17(4):282–305.

Rodrigues, F. C. M., Espadoto, M., Jr, R. H., and Telea, A. (2019). Constructing and visualizing high-quality classifier decision boundary maps. *Information*, 10(9):280–297.

Rodrigues, F. C. M., Jr., R. H., and Telea, A. (2018). Image-based visualization of classifier decision boundaries. In *Proc. SIBGRAPI*.

Schulz, A., Gisbrecht, A., and Hammer, B. (2015). Using discriminative dimensionality reduction to visualize classifiers. *Neural Process. Lett.*, 42(1):27–54.

Schulz, A., Hinder, F., and Hammer, B. (2020). DeepView: Visualizing classification boundaries of deep neural networks as scatter plots using discriminative dimensionality reduction. In Bessiere, C., editor, *Proc. IJCAI*, pages 2305–2311.

Shwartz-Ziv, R. and Tishby, N. (2017). Opening the black box of deep neural networks via information. arXiv:1703.00810 [cs.LG].

Thiyagalingam, J., Shankar, M., Fox, G., and Hey, T. (2022). Scientific machine learning benchmarks. *Nature Reviews Physics*, 4:413–420.

Tzeng, F. Y. and Ma, K.-L. (2005). Opening the black box – data driven visualization of neural networks. In *Proc. IEEE Visualization*.

van der Maaten, L. and Hinton, G. E. (2008). Visualizing data using t-sne. *JMLR*, 9:2579–2605.

van der Zwan, M., Codreanu, V., and Telea, A. (2016). CUBu: Universal real-time bundling for large graphs. *IEEE TVCG*, 22(12):2550–2563.

Venna, J. and Kaski, S. (2006). Visualizing gene interaction graphs with local multidimensional scaling. In *Proc. ESANN*, pages 557–562.

Vernier, E., Comba, J., and Telea, A. (2021). Guided stable dynamic projections. *Computer Graphics Forum*, 40(3):87–98.

Vernier, E., Garcia, R., da Silva, I., Comba, J., and Telea, A. (2020). Quantitative evaluation of time-dependent multidimensional projection techniques. *Computer Graphics Forum*, 39(3):241–252.